

RESEARCH ARTICLE

Variability in spectral absorption within cryptophyte phycobiliprotein types

 Kristiaän A. Merritt¹ | Tammi L. Richardson^{1,2} 
¹Department of Biological Sciences,
University of South Carolina, Columbia,
South Carolina, USA

²School of the Earth, Ocean &
Environment, University of South
Carolina, Columbia, South Carolina, USA
Correspondence
 Tammi L. Richardson, Department of
Biological Sciences, University of South
Carolina, 715 Sumter St., Columbia, SC
29208, USA.

Email: richardson@biol.sc.edu

Funding information
 NSF Division of Environmental Biology,
Grant/Award Number: 1542555

Editor: J. Raven

Abstract

Cryptophytes are known to vary widely in coloration among species. These differences in color arise primarily from the presence of phycobiliprotein accessory pigments. There are nine defined cryptophyte phycobiliprotein (Cr-PBP) types, named for their wavelength of maximal absorbance. Because Cr-PBP type has traditionally been regarded as a categorical trait, there is a paucity of information about how spectral absorption characteristics of Cr-PBPs vary among species. We investigated variability in primary and secondary peak absorbance wavelengths and full width at half max (FWHM) values of spectra of Cr-PBPs extracted from 75 cryptophyte strains (55 species) grown under full spectrum irradiance. We show that there may be substantial differences in spectral shapes within Cr-PBP types, with Cr-Phycocerythrin (Cr-PE) 545 showing the greatest variability with two, possibly three, subtypes, while Cr-PE 566 spectra were the least variable, with only ± 1 nm of variance around the mean absorbance maximum of 565 nm. We provide additional criteria for classification in cases where the wavelength of maximum absorbance alone is not definitive. Variations in spectral characteristics among strains containing the same presumed Cr-PBP type may indicate differing chromophore composition and/or the presence of more than one Cr-PBP in a single cryptophyte species.

KEYWORDS

absorbance, absorption, chromophore, cryptomonad, cryptophyte, phycobilin, phycobiliprotein

INTRODUCTION

Cryptophytes are unicellular, eukaryotic microalgae that are ubiquitous in freshwater, estuarine, and marine environments (Hoef-Emden & Archibald, 2016; Klaveness, 1989). Part of their ecological success is due to their cryptophyte phycobiliprotein (Cr-PBP) accessory pigments that capture wavelengths of light not efficiently absorbed by chlorophylls (Doust et al., 2006), thus allowing them to occupy distinct vertical niches in the water column (Stomp, Huisman, Stahl, et al., 2007; Stomp, Huisman, Vörös, et al., 2007). Cryptophytes are

important primary producers, and their size range (~5–50 μ m) and high digestibility make them attractive prey for grazers (Adolf et al., 2008; Gallegos et al., 2010; Kiili et al., 2009; Klaveness, 1989; Pastoureaud et al., 2003; Pedrós-Alió et al., 1995).

Cryptophytes evolved as the result of a secondary endosymbiosis between an unknown eukaryotic host and a red algal symbiont (Archibald & Keeling, 2002). The general structure of the Cr-PBP is an $\alpha_1\alpha_2\beta\beta$ tetramer with phycobilin chromophores covalently attached to the subunits (Guard-Friar & MacColl, 1986). The β -subunits are believed to have evolved from the

Abbreviations: Cr-PBP, cryptophyte phycobiliprotein; FWHM, full width at half maximum; PBP, phycobiliprotein.

This is an open access article under the terms of the [Creative Commons Attribution-NonCommercial-NoDerivs](https://creativecommons.org/licenses/by-nc-nd/4.0/) License, which permits use and distribution in any medium, provided the original work is properly cited, the use is non-commercial and no modifications or adaptations are made.

© 2024 The Authors. *Journal of Phycology* published by Wiley Periodicals LLC on behalf of Phycological Society of America.

TABLE 1 Cryptophyte PBP chromophore composition and assumed wavelength(s) of absorbance maxima under full spectrum irradiance.

PBP	Chromophores and binding sites				Assumed absorbance max λ (nm)		Example species
	α -Cys-19	β -Cys-50,61	β -Cys-82	β -Cys-158	1°	2°	
Cr-PE 545	DBV	PEB	PEB	PEB	545,	–	<i>Rhodomonas salina</i>
Cr-PE 555	PEB	DBV	PEB	PEB	555,	–	<i>Hemiselmis rufescens</i>
Cr-PE 566	bilin 584 or 618	bilin 584	PEB	bilin 584	566,	–	<i>Cryptomonas ovata</i>
Cr-PC 564	Unknown	Unknown	Unknown	Unknown	564,	618	<i>Hemiselmis aquamarina</i>
Cr-PC 569	PCB	bilin 584	PCB	bilin 584	569,	625	<i>Falcomonas daucooides</i>
Cr-PC 577	PCB	DBV	PCB	PCB	577,	589	<i>Hemiselmis pacifica</i>
Cr-PC 612	PCB	DBV	PCB	PCB	612,	577	<i>Hemiselmis virescens</i>
Cr-PC 630	MBV	DBV	PCB	PCB	630,	583	<i>Chroomonas</i> sp.
Cr-PC 645	MBV	DBV	PCB	PCB	645,	585	<i>Chroomonas mesostigmatica</i>

Note: Cr-PEs have only one absorbance peak. Modified from Richardson (2022) by adding Cr-PC 564 (Magalhães et al., 2021) and including bilin 618 on α -Cys-19 of Cr-PE 566. Some strains of *Cryptomonas ovata* appear to have bilin 584 in this position, while others have bilin 618 (Wedemayer et al., 1992).

β -subunit of a red algal phycoerythrin molecule (Apt et al., 1995). The α -subunits are smaller and are believed to be derived from a red algal linker protein (Rathbone et al., 2021). The β -subunits bind three chromophores, while the α -subunits bind one, all at conserved locations on the protein (Glazer & Wedemayer, 1995). Cryptophyte phycobiliproteins contain six possible phycobilin chromophores (Table 1). Phycoerythrobilin (PEB) and phycocyanobilin (PCB) are both found in red algae and cyanobacteria. Four additional chromophores, 15,16-dihydrobiliverdin (DHBV), bilin 584, bilin 618, and mesobiliverdin (MBV), are unique to cryptophytes (Glazer & Wedemayer, 1995; Wedemayer, 1996; Wedemayer et al., 1992). The chromophores DHBV and MBV are precursors to PEB and PCB, respectively, in their biosynthetic pathways (Frankenberg & Lagarias, 2003; Wedemayer et al., 1992). Bilin 584 and bilin 618 result from synthesis pathways that diverge from the pathways leading to PEB and PCB (Scholes et al., 2012). Chromophore composition, absorption properties, and conformation of the phycobilin-protein complex (e.g., “open” vs. “closed” conformations) all affect the light absorption characteristics of Cr-PBPs (Corbella et al., 2019; Harrop et al., 2014; Michie et al., 2023; Wedemayer, 1996).

To date, there are nine described Cr-PBP types, each named for the presence of a PEB or PCB on the β -Cys-82 binding site and for their wavelength of maximum absorbance in white light (Table 1). Cryptophyte phycoerythrins (Cr-PEs) are red in color, contain a PEB at β -Cys-82, and have a relatively narrow, single absorbance peak near 545 nm, 555 nm, or 566 nm. Cryptophyte phycocyanins (Cr-PCs) are blue-green in color, contain a PCB at β -Cys-82, and often have two absorbance peaks, with the primary peak near 564 nm, 569 nm, 577 nm, 612–615 nm (this varies with species), 630 nm, or 645 nm. Accordingly, the nine currently described Cr-PBPs are Cr-PE 545, Cr-PE 555, Cr-PE 566, Cr-PC 564, Cr-PC 569, Cr-PC 577, Cr-PC 612, Cr-PC 630, and Cr-PC 645 (Hoef-Emden, 2008; Magalhães et al., 2021; Overkamp et al., 2014).

Across the cryptophyte phylogeny, Cr-PE 545 is in multiple clades and is thought to be the ancestral PBP (Greenwold et al., 2019). Cryptophyte phycoerythrins 566, on the other hand, is only in freshwater species of *Cryptomonas* and in one strain of *Baffinella frigidus* (CCMP 2045; Cunningham et al., 2019; Daugbjerg et al., 2018; Greenwold et al., 2019; Hill & Rowan, 1989; Hoef-Emden, 2008). *Hemiselmis* is the most diverse genus with respect to Cr-PBP type, containing species with one of several possible Cr-PEs or Cr-PCs (Cunningham et al., 2019; Hoef-Emden, 2008). *Chroomonas* and *Komma* species group together and only ever have Cr-PC 630 or Cr-PC 645 (Cunningham et al., 2019; Greenwold et al., 2019; Hoef-Emden, 2008). Historically scientists used color (appearance to the human eye) to

classify cryptophytes taxonomically and to group them by “type” (Hill & Rowan, 1989, and references therein). Problems with this approach soon became apparent as scientists realized that color didn't always correlate with other indices of taxonomy (Butcher, 1967), and even the same species could change color if grown in different light or nutrient environments (e.g., Heidenreich & Richardson, 2020; Lane & Archibald, 2008; Vesik & Jeffrey, 1977).

Here, we have characterized variability in spectral absorption across cryptophyte strains with the same presumed Cr-PBP type using a database of absorbance spectra collected by our laboratory. We observed that there could be remarkable variability within a Cr-PBP type with respect to the wavelength of maximum absorbance, the range and shape of the spectral absorbance curve, and whether or not there was a detectable “shoulder” in the spectrum. Our results provide additional criteria for classification in cases where the wavelength of maximum absorbance alone is not definitive. Variations in spectral characteristics among strains containing the same presumed Cr-PBP type may indicate differing chromophore composition and/or the presence of more than one Cr-PBP in a single species, which supports recent evidence of differential gene expression in *Guillardia theta* (over 20 actively expressed α -subunit genes; Kieselbach et al., 2018) and observations that cryptophytes synthesize more than one type of PBP (Rathbone, 2021).

MATERIALS AND METHODS

We measured the absorbance spectra of extracted PBPs from 75 cryptophyte strains, representing at least 14 genera and 55 species (Table 2). Strains were maintained in batch culture at 4, 15, or 20°C on a 12:12h light:dark cycle and an irradiance of 30–90 $\mu\text{moles photons} \cdot \text{m}^{-2} \cdot \text{s}^{-1}$ (exact culture conditions depended on species; see Cunningham et al., 2019 and Heidenreich & Richardson, 2020 for details). Illumination was provided from the side by Daylight Deluxe Arctic White 32-W fluorescent lamps (Philips, Inc.). Stock cultures were transferred to fresh culture media while still in exponential phase and were swirled gently on a daily basis.

We used the freeze/thaw centrifugation method of Lawrenz et al. (2011) as modified by Heidenreich and Richardson (2020) for Cr-PBP extractions. Aliquots (20–50 mL) of midexponential phase culture of each strain were sampled and then centrifuged at 2054 g for 10 min. The resulting supernatant was decanted, the pellet re-suspended in 5 mL of 0.1 M phosphate buffer (pH 6) and homogenized using a vortex mixer, and samples were placed at -20°C for at least 2 h. Once frozen, samples were moved to 5°C to thaw for up to 24 h. Thawed samples were centrifuged at 10,870 g

for 5 min to remove excess cellular debris. The absorbance of each sample extract was measured from 400 to 750 nm at 1-nm intervals with a Shimadzu UV-VIS 2450 dual beam spectrophotometer using a 1-cm quartz glass cuvette against a phosphate buffer blank. Data were scatter-corrected by subtracting absorbance at 750 nm. Duplicate or triplicate measurements made from the same culture served as analytical replicates.

Spectra were analyzed using the pavo package in R and the procspec function to normalize all absorbance data to a scale of 0–1 (Maia et al., 2013, 2019). We then calculated a 3-nm moving slope of the normalized absorbance data to identify areas where slope changed rapidly to identify a “shoulder.” Wavelengths of maximum absorption and measurements of Full Width at Half Maximum (FWHM), defined as spectral width (in nm) at half the maximum absorbance value, were determined for all extracted Cr-PBP spectra. Spectral shapes among species were compared using primary absorption peak, FWHM values, the presence or absence of a shoulder, and the presence or absence of a secondary absorption maximum.

Significant differences among peak wavelengths and FWHM values were analyzed using a Student t -test for unpaired data with unequal variance. Differences were considered significant at $p < 0.01$.

RESULTS

The average primary absorption wavelength of cryptophyte strains with Cr-PE 545 ranged between 540 and 553 nm (Tables 2 and 3). Of the 34 strains from which Cr-PE 545 was extracted, 13 strains had a “normal” single peak (e.g., Figure 1a), 19 had a shoulder at ~ 564 nm (range 560–566 nm, Table 2; Figure 1b), and one, Cr-PE 545 from *Baffinella frigidus* CCMP 2293, had a primary absorption peak at 541 nm and what appeared to be two secondary peaks, one at 592 nm and the other at 643–645 nm (Figure 1c). Thus, within this type of Cr-PBP, there are at least two and possibly three distinct spectral shapes. Full width at half maximum values for this Cr-PBP type ranged from 64 to 75 nm on average (Tables 2 and 3).

For strains that contained Cr-PE 555, spectral shapes were relatively consistent (single peaks with no detectable shoulders), but the location of the primary absorption wavelengths ranged from 548 to 555 nm (average 550 ± 3 nm for $n = 13$ spectra from four strains; Tables 2 and 3, Figure 2a). Strains containing Cr-PE 566 had the lowest observed variability in peak absorption, with a range of 565–566 nm (average 565 ± 1 nm for $n = 53$ spectra from 21 strains) and no detectable shoulders (Figure 2b).

We had only one species each from which to extract Cr-PC 564, Cr-PC 569, and Cr-PC 577. Cryptophyte phycocyanin 564 from *Hemiselmis*

TABLE 2 Strains used in this study.

Strain	PBP	<i>n</i>	1° peak position (nm)	2° peak position (if present) (nm)	Shoulder position (if present) (nm)	FWHM (nm) ± SD
<i>Hemiselms aquamarina</i> RCC 4102	Cr-PC 564	7	566 ± 2	616 ± 1	–	114 ± 4
<i>Hemiselms cryptochromatica</i> CCMP 1181	Cr-PC 569	5	572 ± 1	626 ± 0	–	106 ± 1
<i>Hemiselms pacifica</i> CCMP 706	Cr-PC 577	5	578 ± 0	–	613 ± 2	89 ± 2
<i>Hemiselms tepida</i> CCMP 443	Cr-PC 612	3	612 ± 0	571 ± 0	–	101 ± 0
<i>Hemiselms virescens</i> RCC 3575	Cr-PC 612	4	614 ± 1	577 ± 0	–	90 ± 1
<i>Chroomonas norstedtii</i> NIES 708	Cr-PC 630	1	637	584	–	102
<i>Chroomonas</i> sp. CCAC 0060	Cr-PC 630	3	633 ± 1	583 ± 0	–	102 ± 1
<i>Chroomonas</i> sp. K-1623	Cr-PC 630	1	637	584	–	103
<i>Chroomonas vectensis</i> K-0432	Cr-PC 630	3	631 ± 1	583 ± 0	–	101 ± 2
<i>Komma</i> sp. K-1622	Cr-PC 630	3	631 ± 2 ^a	582 ± 1 ^a	–	110 ± 0
<i>Chroomonas caudata</i> NIES 712	Cr-PC 645	1	647	584	–	103
<i>Chroomonas mesostigmatica</i> CCMP 1168	Cr-PC 645	1	646	585	–	103
<i>Chroomonas</i> sp. CCAC 0059	Cr-PC 645	3	647 ± 0	585 ± 1	–	103 ± 1
<i>Chroomonas</i> sp. CCAC 2291	Cr-PC 645	3	647 ± 0	585 ± 0	–	102 ± 2
<i>Chroomonas</i> sp. CCMP 1221	Cr-PC 645	1	647	584	–	103
<i>Chroomonas</i> sp. CCMP 270	Cr-PC 645	1	646	586	–	103
<i>Baffinella frigidus</i> CCMP 2293	Cr-PE 545	3	542 ± 1	592–595, 645	–	64
<i>Cryptomonas irregularis</i> NIES 698	Cr-PE 545	1	550	–	–	74
<i>Geminigera cryophila</i> CCMP 2564	Cr-PE 545	1	546	–	566	70
<i>Guillardia theta</i> CCMP 327	Cr-PE 545	4	547 ± 1	–	–	66 ± 5
<i>Hanusia phi</i> CCMP 325	Cr-PE 545	1	546	–	–	NA
<i>Hemiselms</i> sp. RCC 2614	Cr-PE 545	3	551 ± 0	–	–	66 ± 5
<i>Proteomonas</i> sp. RCC 1505	Cr-PE 545	3	545 ± 1	–	564 ± 0	72 ± 5
<i>Proteomonas</i> sp. CCMP 2715	Cr-PE 545	1	545	–	564	70
<i>Proteomonas</i> sp. RCC 3072	Cr-PE 545	1	540	–	–	NA
<i>Proteomonas sulcata</i> CCMP 1175	Cr-PE 545	1	548	–	562	65
<i>Rhinomonas reticulata</i> SC-CCAP 995.2	Cr-PE 545	1	552	–	560	65
<i>Rhodomonas abbreviata</i> CCMP 1178	Cr-PE 545	1	551	–	–	66
<i>Rhodomonas atrorosea</i> SC-CCAP 978.6A	Cr-PE 545	1	550	–	–	65
<i>Rhodomonas baltica</i> RCC 350	Cr-PE 545	3	548 ± 1	–	–	NA
<i>Rhodomonas chrysoidea</i> NIES 701	Cr-PE 545	1	549	–	564	66
<i>Rhodomonas falcata</i> NIES 702	Cr-PE 545	1	552	–	–	69
<i>Rhodomonas lens</i> CCMP 739	Cr-PE 545	1	548	–	565	65
<i>Rhodomonas marina</i> K-0435	Cr-PE 545	3	551 ± 2	–	–	69 ± 4
<i>Rhodomonas minuta</i> CPCC 344	Cr-PE 545	1	551	–	565	67
<i>Rhodomonas salina</i> CCMP 1319	Cr-PE 545	4	548 ± 1	–	562 ± 1	70 ± 2
<i>Rhodomonas</i> sp. CCAC 6524B	Cr-PE 545	3	548 ± 1	–	564 ± 1	65 ± 1
<i>Rhodomonas</i> sp. RCC 4444	Cr-PE 545	3	547 ± 1	–	565 ± 1	75 ± 2
<i>Storeatula</i> sp. CCMP 1868	Cr-PE 545	1	548	–	564	65
<i>Storeatula</i> sp. K-1488	Cr-PE 545	3	553 ± 1	–	–	67 ± 2
<i>Teleaulax amphioxieia</i> K-1837	Cr-PE 545	3	547 ± 1	–	563 ± 0	67 ± 1
<i>Teleaulax</i> sp. RCC 4857	Cr-PE 545	3	550 ± 0	–	567 ± 1	68 ± 1
Unidentified sp. CCMP 1179	Cr-PE 545	1	550	–	562	67
Unidentified sp. CCMP 3175	Cr-PE 545	1	545	–	563	71
Unidentified sp. CNOS 0001	Cr-PE 545	3	549 ± 0	–	–	66 ± 1

TABLE 2 (Continued)

Strain	PBP	<i>n</i>	1° peak position (nm)	2° peak position (if present) (nm)	Shoulder position (if present) (nm)	FWHM (nm) ± <i>SD</i>
Unidentified sp. RCC 439	Cr-PE 545	3	549±0	–	–	NA
Unidentified sp. RCC 4474	Cr-PE 545	3	547±1	–	564±0	71±3
Unidentified sp. RCC 4787	Cr-PE 545	3	547±1	–	564±1	68±1
Unidentified sp. RCC 4843	Cr-PE 545	3	548±1	–	565±2	70±4
<i>Urgorri complanatus</i> BEA 0603B	Cr-PE 545	3	547±1	–	562	66
<i>Hemiselmis andersenii</i> CCMP 1180	Cr-PE 555	6	548±0	–	–	59±3
<i>Hemiselmis andersenii</i> CCMP 644	Cr-PE 555	1	554	–	–	54
<i>Hemiselmis rufescens</i> CCMP 440	Cr-PE 555	3	555±1	–	–	53±2
<i>Hemiselmis</i> sp. RCC 4116	Cr-PE 555	3	550±1	–	–	55±3
<i>Cryptomonas borealis</i> CCAC 0113B	Cr-PE 566	3	565±1	–	–	60±4
<i>Cryptomonas commutata</i> CCAC 0109B	Cr-PE 566	1	566	–	–	57
<i>Cryptomonas curvata</i> CCAC 0006	Cr-PE 566	2	565±0	–	–	55±3
<i>Cryptomonas curvata</i> SC-CCAP 979.26	Cr-PE 566	1	566	–	–	54
<i>Cryptomonas erosa</i> CCAC 0740B	Cr-PE 566	3	565±0	–	–	53±1
<i>Cryptomonas loricata</i> CCAC 0189	Cr-PE 566	3	566±0	–	–	53±1
<i>Cryptomonas lucens</i> CCAC 1089B	Cr-PE 566	3	565±0	–	–	59±2
<i>Cryptomonas lucens</i> SC-CCAP 979.35	Cr-PE 566	1	566	–	–	53
<i>Cryptomonas obovoidea</i> CCAC 0184B	Cr-PE 566	6	565±0	–	–	53±2
<i>Cryptomonas obovoidea</i> CCAC 1487B	Cr-PE 566	3	566±0	–	–	54±1
<i>Cryptomonas ovata</i> CCAC 1633B	Cr-PE 566	3	565±0	–	–	57±4
<i>Cryptomonas ovata</i> UTEX 2783	Cr-PE 566	1	566	–	–	55
<i>Cryptomonas phaseolus</i> CCAC 0182B	Cr-PE 566	3	565±0	–	–	53±1
<i>Cryptomonas pyrenoidifera</i> CCMP 1167	Cr-PE 566	1	566	–	–	53
<i>Cryptomonas</i> sp. CCAC 2298	Cr-PE 566	3	566±0	–	–	54±3
<i>Cryptomonas</i> sp. CCAC 2770B	Cr-PE 566	3	566±0	–	–	55±3
<i>Cryptomonas</i> sp. CCAC 3856B	Cr-PE 566	3	566±0	–	–	53±4
<i>Cryptomonas</i> sp. CPCC 336	Cr-PE 566	1	565	–	–	54
<i>Cryptomonas tetrapyrenoidosa</i> CCAC 1800B	Cr-PE 566	3	566±0	–	–	53±1
Unidentified sp. BMFL 0001	Cr-PE 566	3	566±0	–	–	49±1
Unidentified sp. ZIGY 0001	Cr-PE 566	3	565±0	–	–	53±5

Note: Isolations of unarchived strains were done by our lab from water collected at the Baruch Marine Field Lab (BMFL), Georgetown, South Carolina; Battery Park in Charleston, South Carolina (CNOS); and Congaree National Park, South Carolina (ZIGY). FWHM=full width at half maximum=width of the spectrum (nm) at half the maximum absorbance value. NA=not available (used when FWHM could not be reliably determined due to noise); *n*=number of spectra analyzed.

Abbreviations: BEA, Spanish Bank of Algae; CCAC, Central Collection of Algal Cultures at the University of Duisburg-Essen; CCMP, National Center for Marine Algae and Microbiota; CPCC, Canadian Phycological Culture Center; K, Norwegian Culture Collection of Algae; NIES, Microbial Culture Collection at the National Institute for Environmental Studies; RCC, Roscoff Culture Collection; SC-CCAP, Scandinavian Culture Collection of Algae and Protozoa; UTEX, the Culture Collection of Algae at the University of Texas at Austin.

^a*Komma* sp. K-1622 had its primary absorption peak at 582nm and secondary at 631 nm, so we designated the 631 nm peak as “primary” only to follow the conventional “type” designation. See text for details.

aquamarina (Figure 3a) had its primary absorption peak at 566±2nm and a secondary peak at 616±1 nm (*n*=7 spectra), while Cr-PC 569 from *Hemiselmis cryptochromatica* (Figure 3b) had its primary peak at 572±1 nm and secondary peak at 626±0 (*n*=5 spectra), and neither Cr-PBP type had detectable shoulders (Table 2). Cryptophyte phycocyanin 577 from *Hemiselmis pacifica*, however, did

have a detectable shoulder at 613nm (±2 nm; *SD* of *n*=5 spectra) with the primary absorption maximum consistently at 578 nm (Figure 3c).

Hemiselmis tepida and *Hemiselmis virescens* were the only two cryptophytes with Cr-PC 612/615 (Figure 4). Although they are both categorized as having Cr-PC 612/615 using their primary absorption maxima (612 and 614 nm, respectively, see Table 2), the

TABLE 3 Ranges for averages of Primary Absorbance Peaks and Full Width at Half Maximum (FWHM) values.

PBP type	Number of spectra analyzed	Number of species (#strains)	Range of strain averages for primary absorbance peak (nm)	Range of strain averages for FWHM (nm)
Cr-PE 545	$n=69$	34 (34)	540–553	64–75
Cr-PE 555	$n=13$	3 (4)	548–555	53–59
Cr-PE 566	$n=53$	17 (21)	565–566	49–60
Cr-PC 564	$n=7$	1 (1)	566	114
Cr-PC 569	$n=5$	1 (1)	572	106
Cr-PC 577	$n=5$	1 (1)	578	89
Cr-PC 612	$n=5$	2 (2)	612–614	90–101
Cr-PC 630	$n=11$	5 (5)	631–637 ^a	101–103 ^b
Cr-PC 645	$n=10$	6 (6)	646–647	102–103

Note: Single values indicate there was only one species analyzed for that cryptophyte phycoerythrin (Cr-PE) or cryptophyte phycocyanin (Cr-PC). Ranges consider all spectra collected and are not weighted by number of spectra collected per species.

^aRange assumes that 631 nm is the primary absorbance peak for *Komma* sp. K-1622 (by convention); however, its true primary peak was at 582 ± 1 nm. See Table 2 and text for details.

^bDoes not include *Komma* sp.

positions of their secondary peak were significantly different (571 and 577 nm, respectively), resulting in an 11 nm difference in FWHM (Tables 2 and 3).

Strains with Cr-PC 630 showed relatively low variability in primary and second absorption maxima and FWHM (Figure 5a), with the exception of *Komma* sp. (Figure 5b) and possibly *Chroomonas* sp. K-1623, but we had only one spectrum for that species. Our data for *Komma* sp. ($n=3$ spectra) showed the primary peak at 582 nm and secondary peak at 631 nm (Table 2). By convention, we classified this species as a Cr-PC 630 type, despite the 582 nm peak, because the primary and secondary peak heights were less than 3% different and because its FWHM (110 ± 0 nm) was closest to the FWHM for other Cr-PC 630 strains (Table 2).

All cryptophytes with Cr-PC 645 used in our study were thought to be in the genus *Chroomonas* based on their culture collection designations (six strains, but note that Hoef-Emden, 2018, has revised this genus substantially). Primary absorption peaks for all strains were at 646 or 647 nm, had secondary peaks between 584 and 586 nm, and had FWHM values that were consistently 102–103 nm (Tables 2 and 3, Figure 6). In general, Cr-PE 555 and 566 spectra had narrow FWHMs (53–59 nm and 49–60 nm, respectively), while those of Cr-PC 630 spectra were widest (101–110 nm; Table 3).

DISCUSSION

The inspiration for this work came from an earlier study by Hill and Rowan (1989), who summarized primary and secondary absorbance peak locations, absorbance shoulders, and fluorescence emission peaks for values from the literature and for data they collected on 26 cryptophyte strains (~23 species). Of the ~39 species on which they reported, 11 were also analyzed in this

study (Table 4), with several differences. We did not detect shoulders in our strains of *Rhodomonas atrosea* or *Rhodomonas baltica*, as did Ó hEocha et al. (1964) and Hill and Rowan (1989), respectively, nor in our two strains of *Cryptomonas ovata*, as did MacColl et al. (1976). Hoef-Emden and Melkonian (2003) later showed that the “*C. ovata*” used by MacColl et al. (1976; CCAP 979/61) was instead *C. pyrenoidifera*, which explains this discrepancy.

Our values for peak absorbance of *Rhodomonas salina* and *R. lens* were closer to 548 nm than to 545 nm as observed in different strains of these species by others (Haxo & Fork, 1959; Hill & Rowan, 1989; MacColl et al., 1976, 1983; Stewart & Farmer, 1984). Our classification of *Hemiselmis virescens* as a Cr-PC 612/615 type agrees with earlier studies (Glazer & Cohen-Bazire, 1975; MacColl & Guard-Friar, 1983; Ó hEocha et al., 1964; Ó hEocha & Raftery, 1959), but measurements by others on the Millport 64 strain of *H. virescens* differed substantially, resulting in it being classified as a Cr-PC 645 type by some (Table 4, see Allen et al., 1959; Glazer & Cohen-Bazire, 1975; Ó hEocha et al., 1964). Another major difference is that we classified our strain of *Chroomonas vectensis* as a Cr-PC 630 type based on its absorbance maximum (631 ± 1 nm), whereas Hill and Rowan's (1989) strain had a primary peak at 645 nm, so they deemed it a Cr-PC 645 type. Measurements of FWHM on our strain (101 ± 2 nm) were similar to other Cr-PC 630 types we studied but were also not significantly different from FWHM values for the Cr-PC 645 types. So, in this case, FWHM did not help with classifying the PBP in this species to type. In general, these comparisons illustrate the difficulty in determining Cr-PBP type where there is substantial variability in spectral characteristics even among strains of the same species.

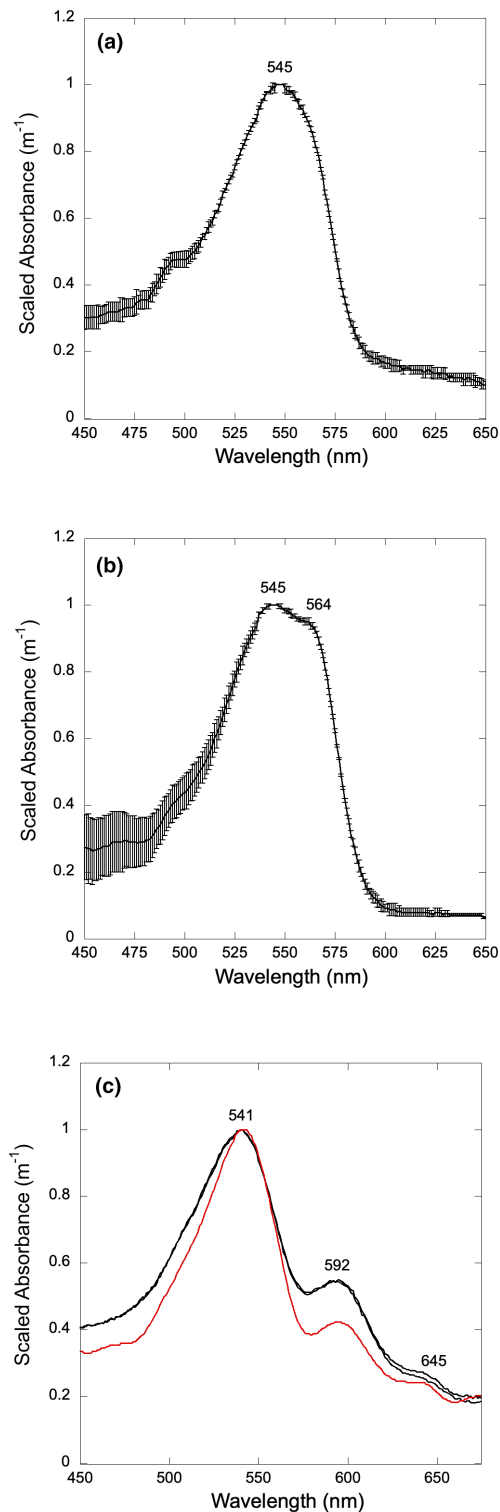


FIGURE 1 Scaled absorbance spectra for Cr-PE 545 from (a) *Guillardia theta* CCMP 327, (b) *Proteomonas* sp. RCC 1505, and (c) *Baffinella frigidus* CCMP 2293. Error bars represent the means and standard deviations of $n=4$ of *G. theta* and $n=3$ of *Proteomonas* sp. For *B. frigidus*, there are duplicate spectra for new cultures acquired in October 2023, and one replicate of an older culture for which a spectrum was measured in May 2020.

Hill and Rowan (1989) stated that in Cr-PE 545, the “distinct shoulder in the absorption spectrum at ~ 563 nm clearly distinguishes this type from Cr-phycoerythrins 555 and 566” (p. 460), and as stated, Cr-PE 545 from all the strains they studied had shoulders. We observed 19 Cr-PE 545 strains with shoulders but also observed 13 strains without shoulders for which the absorbance maxima classified them as a Cr-PE 545 type, as did the FWHM values, which were significantly different from the FWHMs of Cr-PE 555 and 566. Further, Cr-PE 545 from *Baffinella frigidus* CCMP 2293, exhibited a possible third subtype, with an absorbance maximum at ~ 541 nm and two secondary peaks, one at ~ 592 nm and the second at ~ 645 nm. In our database, we had only one spectrum for this species (collected in May 2020), so we purchased a new aliquot from the NCMA, extracted its PBPs, and ran two additional spectra in October 2023. The wavelengths of maximum absorbance of the old and new cultures match almost exactly, as do the secondary peaks. Notable was the difference in peak height of the old versus new cultures; the new cultures had higher absorbance near 592 nm but less distinct absorbance at 645 nm. The reason for this is not clear.

Although we had only one species with this subtype of Cr-PE 545 absorbance spectrum in our study, both *Chroomonas* sp. CS24 (Martin & Hiller, 1987) and *Cryptomonas acuta* (Hill & Rowan, 1989) have similar spectra. *Chroomonas* sp. had a primary peak at 545 nm, a shoulder at 564 nm, and a secondary peak at 645 nm. Further, absorbance spectra on separated and purified subunits showed strong absorption at 644 nm by the α -subunit fraction (Martin & Hiller, 1987). *Cryptomonas acuta* also had peak absorbance at 545 nm (but no shoulder) and a secondary peak at 645 nm and had fluorescence emission characteristics typical of a Cr-PE 545 type (Hill & Rowan, 1989).

Though consistent in spectral shape, there was a wide range in absorbance maxima for *Hemiselmis* species with Cr-PE 555, the only genus we had with this PBP. Cryptophyte phycoerythrin extracted from *H. andersenii* CCMP 1180 had its peak absorbance consistently at 548 nm, which, using the Hill and Rowan (1989) criterion, might classify it as a Cr-PE 545 type instead of Cr-PE 555. This ambiguity was also noted by Hoef-Emden (2008) and led her to designate its type as “PE 545/555.” Although the primary absorbance peak of *Hemiselmis andersenii* CCMP 1180 was closer to a Cr-PE 545 type, its average FWHM was closer to that of the other Cr-PE 555 *Hemiselmis* strains and different than other Cr-PE types. Thus, we have kept its classification as Cr-PE 555. Conversely, *Hemiselmis* sp. RCC 2614 had a primary absorbance peak at 551 nm, so we

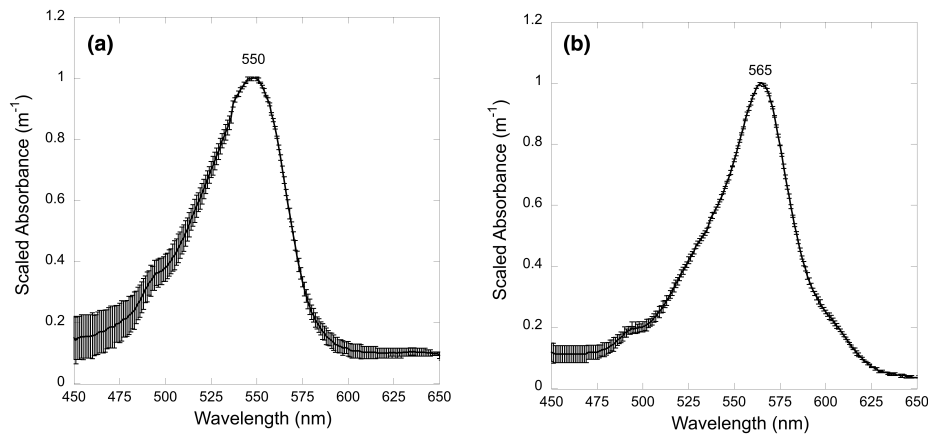


FIGURE 2 Scaled absorbance spectra for (a) Cr-PE 555 from *Hemiselmis andersenii* CCMP 1180, and (b) Cr-PE 566 from *Cryptomonas phaseolus* CCAC 0182B. Error bars represent the means and standard deviations for $n=6$ and $n=3$ replicates for *H. andersenii* and *C. phaseolus*, respectively.

could classify it as a Cr-PE 555 strain, but its FWHM (66 ± 5 nm) was closer to Cr-PE 545-containing strains. Thus, we have classified it as a Cr-PE 545 type. The nonoverlapping nature of FWHM values for the three Cr-PE types (and significant differences among them) makes this a useful parameter for the classification of these PBPs.

We had spectra from only one species each for Cr-PC 564, Cr-PC 569, and Cr-PC 577; thus it was not possible for us to investigate whether there was interstrain or species variability. In the study that first identified *Hemiselmis aquamarina* and characterized Cr-PC 564, two strains were isolated, one from marine waters off Brazil (BMAK265) and the other from Japan (RCC4102; used in this study; Magalhães et al., 2021). Small variations in spectral absorption were observed: BMAK265 had an absorbance maximum at 564 nm and a secondary peak between 616 and 620 nm, whereas RCC4102 had a maximum that ranged between 557 and 566 nm and a secondary peak from 616 to 619 nm (Magalhães et al., 2021; see their figure 3). Our data agreed with these results (primary peak at 566 ± 2 nm, secondary at 616 ± 1 nm). We note from the Magalhães et al. (2021) figure, however, that the secondary peak of RCC4102 appears lower in magnitude relative to the secondary peak of BMAK265. No units are provided on the y-axis of that figure, but if we assume that spectra for both strains are scaled the same for comparison, the lower absorption at ~ 618 nm may reflect differences in chromophore content or conformation. (To our knowledge, the chromophores of Cr-PC 564 have not yet been characterized.) A similar reasoning may explain differences in secondary peak absorbance that we observed for *Baffinella frigidus*, as mentioned earlier.

We had only one species from which to isolate Cr-PC 569 (*Hemiselmis cryptochromatica*) and Cr-PC 577 (*Hemiselmis pacifica*). Hill and Rowan (1989) were the first to isolate Cr-PC 569; they isolated it from *Chroomonas* (now *Falcomonas*) *daucoides*.

Wedemayer (1996) later characterized its phycobilin composition in detail (as shown in Table 1). In their original description of *H. cryptochromatica*, Lane and Archibald (2008) reported a maximum absorbance peak at 630 nm (not 569 nm) for the same strain as was used in our study (CCMP 1181). They also noted that their cells were “lacking color to faint gray” in appearance (Lane & Archibald, 2008, p. 442). We have assumed that our cultures of *H. cryptochromatica* contain Cr-PC 569 based on measurements made in our laboratory (Cunningham et al., 2019), but we also observed that *H. cryptochromatica* varied greatly in color depending on the color of light in which they were grown and did so in a manner complementary to the color of light in their environment (they exhibited “chromatic acclimation,” see Heidenreich & Richardson, 2020). So, contradictory reports of wavelength maxima can perhaps be explained by the spectral output of the lights under which *H. cryptochromatica* (or any cryptophyte) is grown.

Spangler et al. (2022) compared green light-acclimated and nonacclimated *Hemiselmis pacifica* and observed that neither the protein sequences nor the protein structures in Cr-PC 577 were modified by chromatic acclimation. They concluded that the spectral absorbance shift response observed by Heidenreich and Richardson (2020) must be due to a change in “one chromophore on the β -subunit” (Spangler et al., 2022, p. 340). However, this conclusion was not based on direct characterization of chromophores.

Spectral variation in Cr-PBP absorption may result not only from chromophore composition but also from changes in conformation of the quaternary structures (“open” versus “closed” conformations; see Harrop et al., 2014) or interactions between individual chromophores and the α -subunits (Michie et al., 2023). Unlike the β -subunit, which is encoded by a single gene on the plastid genome (Douglas, 1992), the α -subunits are encoded by multiple genes, all of which

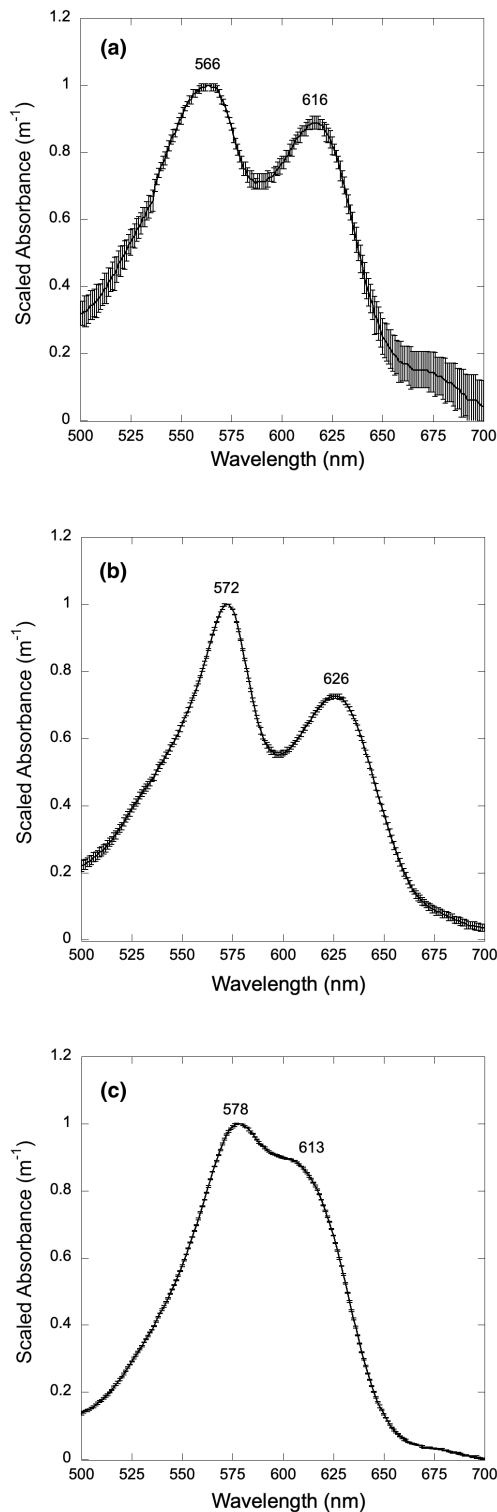


FIGURE 3 Scaled absorbance spectra for (a) Cr-PC 564 from *Hemiselmis aquamarina* RCC 4102, (b) Cr-PC 569 from *Hemiselmis cryptochromatica* CCMP 1181, and (c) Cr-PC 577 from *Hemiselmis pacifica* CCMP 706. Error bars represent means and standard deviations for $n=7$ (*H. aquamarina*), $n=5$ (*H. cryptochromatica*), and $n=5$ (*H. pacifica*) replicates.

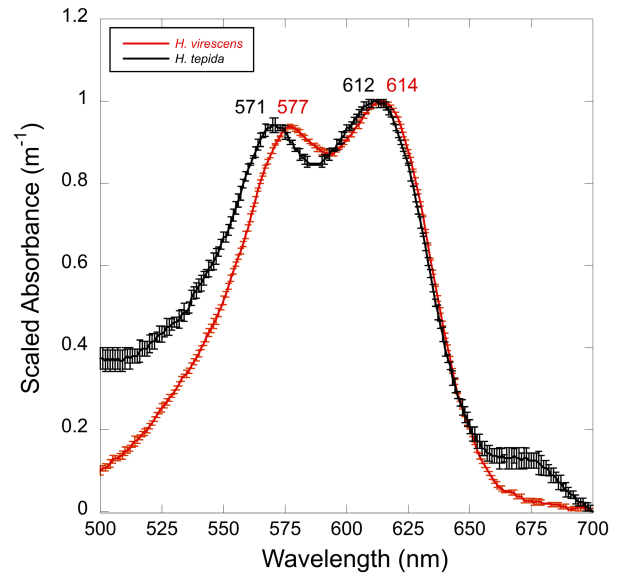


FIGURE 4 Scaled absorbance spectra for Cr-PC 612/615 extracted from *Hemiselmis virescens* RCC 3575 and *Hemiselmis tepida* CCMP 443. Error bars represent means and standard deviations of $n=4$ and $n=3$ replicates for *H. virescens* and *H. tepida*, respectively. The primary absorption wavelength did not differ significantly between these species, but the location of the secondary maximum was significantly different (unpaired Student t -test, $p < 0.001$).

are in the nuclear genome (Curtis et al., 2012). The α -subunits control the quaternary structure of the Cr-PBPs (Harrop et al., 2014), the ability of the Cr-PBP to move into the thylakoid, and even the orientation of chromophores on the β -subunit (Michie et al., 2023). Although cryptophytes are thought to only have a single PBP type per species, some have been shown to express up to 20 distinct α -subunits (*Guillardia theta* in Kieselbach et al., 2018, multiple species in Michie et al., 2023). Michie et al. (2023) observed that the β -subunits of *Hemiselmis pacifica* and *H. virescens* were nearly identical in structure and sequence, but the α -subunits had little sequence similarity. Further, even small differences in amino acid sequences could result in shifts of primary and secondary absorbance peaks. They also observed that four *Hemiselmis* species (*H. andersenii*, *H. rufescens*, *H. tepida*, and *H. virescens*) expressed genes for both closed-form and open-form α -subunits. Thus, differential expression of the α -subunit genes could potentially account for the spectral variability seen in Cr-PBPs, especially in *Hemiselmis*.

Our approach to measuring the absorption of light by Cr-PBPs—extraction in buffer followed by bulk spectroscopy—was not intended or designed to

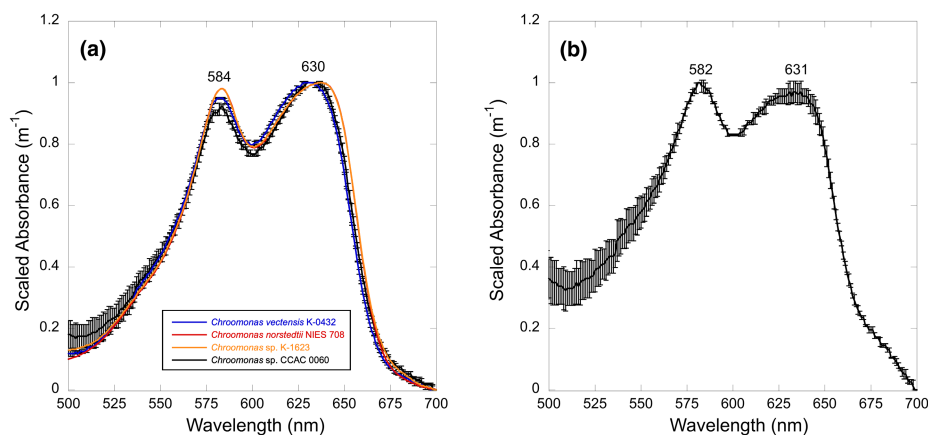


FIGURE 5 Scaled absorbance spectra for Cr-PC 630 extracted from (a) *Chroomonas vectensis* K-0432 ($n=3$), *Chroomonas norstedtii* NIES 708 ($n=1$), *Chroomonas* sp. K-1623 ($n=1$), and *Chroomonas* sp. CCAC 0060 ($n=3$), and (b) *Komma* sp. K-1622 ($n=3$). Error bars indicate means and standard deviations of replicate samples for species with $n=3$. There was no significant difference in primary and secondary peak heights in *Komma* sp., but note the variability in height of the 631 nm peak.

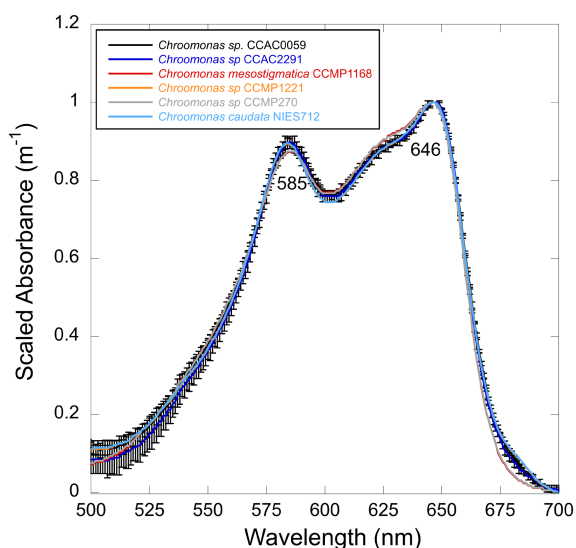


FIGURE 6 Scaled absorbance spectra for Cr-PC 645 extracted from six species of *Chroomonas*. Error bars indicate the means and standard deviations for $n=3$ replicates of *Chroomonas* sp. CCAC 0059 and $n=3$ replicates of *Chroomonas* sp. CCAC 2291. *Chroomonas* sp. CCMP 270, *Chroomonas* sp. CCMP 1221, *Chroomonas mesostigmatica* CCMP 1168, and *Chroomonas caudata* NIES 712 have $n=1$ only.

detect multiple α -subunits or to determine whether, contrary to conventional thought, cryptophytes actually have more than one type of assembled PBP. This latter possibility was raised in the doctoral thesis work of Rathbone (2021). Rathbone noted that the idea of “one PBP per cryptophyte species” is prevalent in the literature despite evidence presented early on that this may not be the case (e.g., see Allen et al., 1959; Mörschel & Wehrmeyer, 1977)

and has likely persisted in the literature because one PBP type usually dominates the Cr-PBP pool. Using sophisticated and sensitive ion chromatography, the resulting publication Rathbone et al. (2023) showed that in *Hemiselmis andersenii*, three PBP “spectrotypes” exist: *HaPE555*, *HaPE560*, and *HaPE645* (where *Ha* indicates *H. andersenii*). Each spectrotpe is composed of two $\alpha\beta$ protomers but differs with respect to α -subunit sequences, which results in differing quaternary structures and thus variations in spectral absorption. Notably, *HaPE645* has differing chromophores (one PCB and one PEB) on its β -subunits, resulting in substantially different absorption properties. Of relevance to this study, Rathbone (2021) stated that it is “possible that the levels of all of these PBPs are regulated by environmental conditions such as light colour and intensity” (p. 180).

The variability we observed and others have observed in Cr-PBP absorbance spectra among species with the same Cr-PBP “type” and among strains of the same species may thus reflect underlying differences in chromophore composition and orientation, conformation of the Cr-PBP molecules themselves, or even relative differences in Cr-PBP type and content. There may be a phylogenetic link in that the greatest variability we documented was within what we believe is the ancestral Cr-PBP type, Cr-PE 545. All of these are influenced by the cryptophyte's light environment, but the specific relationships are yet to be determined. As our knowledge base grows, if we wish to continue to classify cryptophytes according to PBP “type,” then using additional measures such as FWHM values may be useful, especially for the Cr-PEs that have relatively narrow ranges of FWHM values that differ significantly among types.

TABLE 4 Summary of spectral characteristics on species in common between Hill and Rowan (1989) and this study (in bold).

Species	Source or strain	Primary peak	Shoulder	Secondary peak	Cr-PBP "type"
<i>Rhodomonas atrosea</i>	Butcher	¹ 542	560–570	–	Cr-PE 545
<i>Rhodomonas atrosea</i>	SC-CAP 978.6A	550	–	–	Cr-PE 545
<i>Rhodomonas baltica</i>	MUCC Cr 025	544	562	–	Cr-PE 545
<i>Rhodomonas baltica</i>	RCC 350	548 ± 1	–	–	Cr-PE 545
<i>Rhodomonas lens</i>	Provasoli	² 545	–	–	Cr-PE 545
<i>Rhodomonas lens</i>	Provasoli	³ 545	560	–	Cr-PE 545
<i>Rhodomonas lens</i>	Provasoli	⁴ 544	560	–	Cr-PE 545
<i>Rhodomonas lens</i>	CCMP 739	548	565	–	Cr-PE 545
<i>Rhodomonas salina</i>	Guillard	⁵ 545	–	–	Cr-PE 545
<i>Rhodomonas salina</i>	MUCC Cr 043	542	564	–	Cr-PE 545
<i>Rhodomonas salina</i>	MUCC Cr 044	545	562	–	Cr-PE 545
<i>Rhodomonas salina</i>	CCMP 1319	548 ± 1	562 ± 1	–	Cr-PE 545
<i>Proteomonas sulcata</i>	MUCC Cr 08	549 ^a	564 ^a	–	Cr-PE 545
<i>Proteomonas sulcata</i>	CCMP 1175	548	562	–	Cr-PE 545
<i>Hemiselmis rufescens</i>	Plymouth D	⁶ 556	–	–	Cr-PE 555
<i>Hemiselmis rufescens</i>	Plymouth D	¹ 556	–	–	Cr-PE 555
<i>Hemiselmis rufescens</i>	CCMP 440	555 ± 1	–	–	Cr-PE 555
<i>Cryptomonas ovata</i>	CCAP 979/3	³ 566	600	–	Cr-PE 566
<i>Cryptomonas ovata</i>	CCAC 1633B	565 ± 0	–	–	Cr-PE 566
<i>Cryptomonas ovata</i>	UTEX 2783	566	–	–	Cr-PE 566
<i>Cryptomonas tetrapyrenoidosa</i>	MUCC Cr 068	566	–	–	Cr-PE 566
<i>Cryptomonas tetrapyrenoidosa</i>	CCAC 1800B	566 ± 0	–	–	Cr-PE 566
<i>Hemiselmis virescens</i>	Plymouth 157	⁶ 615	–	577	Cr-PC 615
<i>Hemiselmis virescens</i>	Plymouth 157	¹ 615	–	585	Cr-PC 615
<i>Hemiselmis virescens</i>	Plymouth 157	⁹ 612	–	577	Cr-PC 612
<i>Hemiselmis virescens</i>	Plymouth 157	⁷ 612	–	585	Cr-PC 612
<i>Hemiselmis virescens</i>	RCC 3575	614 ± 1	–	577 ± 0	Cr-PC 615
<i>Hemiselmis virescens</i>	Millport 64	⁸ 645	625	580	Cr-PC 645
<i>Hemiselmis virescens</i>	Millport 64	¹ 643	625	583	Cr-PC 645
<i>Hemiselmis virescens</i>	Millport 64	⁹ 641	–	581	Cr-PC 645
<i>Chroomonas vectensis</i>	MUCC Cr 019	645	625	582	Cr-PC 645
<i>Chroomonas vectensis</i>	K-0432	631 ± 1	–	583 ± 0	Cr-PC 630
<i>Chroomonas mesostigmatica</i>	Butcher	¹ 643	–	583	Cr-PC 645
<i>Chroomonas mesostigmatica</i>	NEPCC 470	645	625	582	Cr-PC 645
<i>Chroomonas mesostigmatica</i>	CCMP 1168	646	–	585	Cr-PC 645

Note: Measurements are by Hill and Rowan (1989) unless otherwise indicated. ¹Ó hEocha et al. (1964), ²Haxo and Fork (1959), ³MacColl et al. (1976), ⁴MacColl et al. (1983), ⁵Stewart and Farmer (1984), ⁶Ó hEocha and Raftery (1959), ⁷MacColl and Guard-Friar (1983), ⁸Allen et al. (1959), ⁹Glazer and Cohen-Bazire (1975).

Abbreviation: MUCC, Melbourne University Culture Collection.

^aDiplomorph form of *Proteomonas sulcata*.

CONCLUSIONS

We investigated variability in primary and secondary peak absorbance wavelengths and FWHM values of spectra of Cr-PBPs extracted from 75 cryptophyte strains (55 species) grown under full spectrum irradiance. We showed that there may be substantial

differences in spectral shapes within Cr-PBP types, with Cr-Phycoerythrin (Cr-PE) 545 showing the greatest variability with two, and possibly three, subtypes, while Cr-PE 566 spectra were the least variable, with only ±1 nm of variance around the mean absorbance maximum of 565 nm. All FWHM values differed significantly among the Cr-PE types we examined and may

help distinguish among Cr-PE types when primary absorbance maxima are inconclusive. Variability among species or strains with the same presumed Cr-PBP (especially within Cr-PE 545 types) may indicate differing chromophore composition and/or the presence of more than one Cr-PBP in a single cryptophyte species, which in turn may reflect the light and/or nutrient history of that strain.

AUTHOR CONTRIBUTIONS

Kristiaän A. Merritt: Conceptualization (lead); formal analysis (lead); investigation (equal); writing – original draft (lead). **Tammi Richardson:** Conceptualization (equal); data curation (equal); formal analysis (supporting); funding acquisition (lead); project administration (lead); resources (lead); writing – review and editing (lead).

ACKNOWLEDGMENTS

The authors wish to thank Jared Rose, Cameron Riddick, and Abigail Davis for technical assistance. We are grateful to the National Science Foundation's Dimensions of Biodiversity Program (DEB1542555 to TLR and Jeffrey L. Dudycha) for funding. Comments from two perspicacious reviewers substantially improved the manuscript. The authors declare no conflicts of interest.

FUNDING INFORMATION

National Science Foundation DEB1542555 to TLR and Jeffrey L. Dudycha.

ORCID

Tammi L. Richardson  <https://orcid.org/0000-0002-0667-3455>

REFERENCES

- Adolf, J. E., Bachvaroff, T., & Place, A. R. (2008). Can cryptophyte abundance trigger toxic *Karlodinium veneficum* blooms in eutrophic estuaries? *Harmful Algae*, 8, 119–128.
- Allen, M. B., Dougherty, E. C., & McLaughlin, J. J. A. (1959). Chromoprotein pigments of some cryptomonad flagellates. *Nature*, 184, 1047–1049.
- Apt, K. E., Collier, J. L., & Grossman, A. R. (1995). Evolution of the phycobiliproteins. *Journal of Molecular Biology*, 248, 79–96.
- Archibald, J. M., & Keeling, P. J. (2002). Recycled plastids: A “green movement” in eukaryotic evolution. *Trends in Genetics*, 18, 577–584.
- Butcher, R. W. (Ed.). (1967). An introductory account of the smaller algae of British coastal waters. Part IV. Cryptophyceae. In *Fishery investigations*, series IV. Her Majesty's Stationary Office.
- Corbella, M., Cupellini, L., Lipparini, F., Scholes, G. D., & Curutchet, C. (2019). Spectral variability in phycocyanin cryptophyte antenna complexes is controlled by changes in the α -polypeptide chains. *ChemPhotoChem*, 3, 945–956.
- Cunningham, B. R., Greenwold, M. J., Lachenmyer, E. M., Heidenreich, K. M., Davis, A. C., Dudycha, J. L., & Richardson, T. L. (2019). Light capture and pigment diversity in marine and freshwater cryptophytes. *Journal of Phycology*, 55, 552–564.
- Curtis, B. A., Tanifuji, G., Burki, F., Gruber, A., Irimia, M., Maruyama, S., Arias, M. C., Ball, S. G., Gile, G. H., Hirakawa, Y., Hopkins, J. F., Kuo, A., Rensing, S. A., Schmutz, J., Symeonidi, A., Elias, M., Eveleigh, R. J. M., Herman, E. K., Klute, M. J., ... Archibald, J. M. (2012). Algal genomes reveal evolutionary mosaicism and the fate of nucleomorphs. *Nature*, 492, 59–65.
- Daugbjerg, N., Norlin, A., & Lovejoy, C. (2018). *Baffinella frigidus* gen. Et Sp. Nov. (Baffinellaceae fam. Nov., Cryptophyceae) from Baffin Bay: Morphology, pigment profile, phylogeny and growth rate response to three abiotic factors. *Journal of Phycology*, 54, 665–680.
- Douglas, S. E. (1992). Eukaryote-eukaryote endosymbioses: Insights from studies of a cryptomonad alga. *Biosystems*, 28, 57–68.
- Doust, A. B., Wilk, K. E., Curmi, P. M. G., & Scholes, G. D. (2006). The photophysics of cryptophyte light harvesting. *Journal of Photochemistry and Photobiology*, 184, 1–17.
- Frankenberg, N., & Lagarias, J. C. (2003). Phycocyanobilin:Ferredoxin oxidoreductase of *anabaena* sp. PCC 7120. Biochemical and spectroscopic characterization. *Journal of Biological Chemistry*, 278, 9219–9226.
- Gallegos, C. L., Jordan, T. E., & Hedrick, S. S. (2010). Long-term dynamics of phytoplankton in the Rhode River, Maryland. *Estuaries and Coasts*, 33, 471–484.
- Glazer, A. N., & Cohen-Bazire, G. (1975). A comparison of cryptophycocyanins. *Archives of Microbiology*, 104, 29–32.
- Glazer, A. N., & Wedemayer, G. J. (1995). Cryptomonad biliproteins – An evolutionary perspective. *Photosynthesis Research*, 46, 93–105.
- Greenwold, M. J., Cunningham, B. R., Lachenmyer, E. M., Pullman, J. M., Richardson, T. L., & Dudycha, J. L. (2019). Diversification of light capture ability was accompanied by the evolution of phycobiliproteins in cryptophyte algae. *Proceedings of the Royal Society B*, 286, 20190655.
- Guard-Friar, D., & MacColl, R. (1986). Subunit separation (α , α' , β) of cryptomonad biliproteins. *Photochemistry and Photobiology*, 43, 81–85.
- Harrop, S. J., Wilk, K. E., Dinshaw, R., Collini, E., Mirkovic, T., Teng, C. Y., Oblinsky, D. G., Green, B. R., Hoef-Emden, K., Hiller, R. G., Scholes, G. D., & Curmi, P. M. G. (2014). Single-residue insertion switches the quaternary structure and exciton states of cryptophyte light-harvesting proteins. *Proceedings of the National Academy of Sciences of the United States of America*, 111, E2666–E2675.
- Haxo, F. T., & Fork, D. C. (1959). Photosynthetically active accessory pigments of cryptomonads. *Nature*, 184, 1051–1052.
- Heidenreich, K. M., & Richardson, T. L. (2020). Photopigment, absorption, and growth responses of marine cryptophytes to varying spectral irradiance. *Journal of Phycology*, 56, 507–520.
- Hill, D. R. A., & Rowan, K. S. (1989). The biliproteins of the Cryptophyceae. *Phycologia*, 28, 455–463.
- Hoef-Emden, K. (2008). Molecular phylogeny of phycocyanin-containing cryptophytes: Evolution of biliproteins and geographical distribution. *Journal of Phycology*, 44, 985–993.
- Hoef-Emden, K. (2018). Revision of the genus *Chroomonas* Hansgirg: The benefits of DNA-containing specimens. *Protist*, 169, 662–681.
- Hoef-Emden, K., & Archibald, J. M. (2016). Cryptophyta (cryptomonads). In J. M. Archibald, A. G. B. Simpson, C. H. Slamovits, L. Margulis, M. Melkonian, D. J. Chapman, & J. O. Corliss (Eds.), *Handbook of the protists*. Springer International.
- Hoef-Emden, K., & Melkonian, M. (2003). Revision of the genus *Cryptomonas* (Cryptophyceae): A combination of molecular phylogeny and morphology provides insights into a long-hidden dimorphism. *Protist*, 154, 371–409.

- Kieselbach, T., Cheregi, O., Green, B. R., & Funk, C. (2018). Proteomic analysis of the phycobiliprotein antenna of the cryptophyte alga *Guillardia theta* cultured under different light intensities. *Photosynthesis Research*, *135*, 149–163.
- Kiili, M., Pulkkanen, M., & Salonen, K. (2009). Distribution and development of under-ice phytoplankton in 90-m deep water column of Lake Päijänne (Finland) during spring convection. *Aquatic Ecology*, *43*, 707–713.
- Klaveness, D. (1989). Biology and ecology of the cryptophyceae: Status and challenges. *Biological Oceanography*, *6*(3–4), 257–270.
- Lane, C. E., & Archibald, J. M. (2008). New marine members of the genus *Hemiselmis* (Cryptomonadales, Cryptophyceae). *Journal of Phycology*, *44*, 439–450.
- Lawrenz, E., Fedewa, E. J., & Richardson, T. L. (2011). Extraction protocols for the quantification of phycobilins in aqueous phytoplankton extracts. *Journal of Applied Phycology*, *23*(5), 865–871.
- MacColl, R., Berns, D. S., & Gibbons, O. (1976). Characterization of cryptomonad phycoerythrin and phycocyanin. *Archives of Biochemistry and Biophysics*, *177*, 265–275.
- MacColl, R., & Guard-Friar, D. (1983). Phycocyanin 612: A biochemical and biophysical study. *Biochemistry*, *22*, 5568–5572.
- MacColl, R., Guard-Friar, D., & Castorday, K. (1983). Chromatographic and spectroscopic analysis of phycoerythrin 545 and its subunits. *Archives of Microbiology*, *135*, 194–198.
- Magalhães, K., Santos, A. L., Vaulot, D., & Oliveira, M. C. (2021). *Hemiselmis aquamarina* sp. nov. (Cryptomonadales, Cryptophyceae), a cryptophyte with a novel phycobilin type (Cr-PC 564). *Protist*, *172*, 125832.
- Maia, R., Eliason, C. M., Bitton, P. P., Doucet, S. M., & Shawkey, M. D. (2013). pavo: An R package for the analysis, visualization and organization of spectral data. *Methods in Ecology and Evolution*, *4*(10), 906–913.
- Maia, R., Gruson, H., Endler, J. A., & White, T. E. (2019). pavo2: New tools for the spectral and spatial analysis of colour in R. *Methods in Ecology and Evolution*, *10*(7), 1097–1107.
- Martin, C. D., & Hiller, R. G. (1987). Subunits and chromophores of a type I phycoerythrin from a *Chroomonas* sp. (Cryptophyceae). *Biochimica et Biophysica Acta*, *923*, 88–97.
- Michie, K. A., Harrop, S. J., Rathbone, H. W., Wilk, K. E., Teng, C. Y., Hoef-Emden, K., Hiller, R. G., Green, B. R., & Curmi, P. M. G. (2023). Molecular structures reveal the origin of spectral variation in cryptophyte light harvesting antenna proteins. *Protein Science*, *32*, e4586.
- Mörschel, E., & Wehrmeyer, W. (1977). Multiple forms of phycoerythrin-545 from *Cryptomonas maculata*. *Archives of Microbiology*, *113*, 83–89.
- Ó hEocha, C., Ó Carra, P. O., & Mitchell, D. (1964). Biliproteins of cryptomonad algae. *Proceedings of the Royal Irish Academy*, *63B*, 191–200.
- Ó hEocha, C., & Raftery, M. (1959). Phycoerythrins and phycocyanins of cryptomonads. *Nature*, *184*, 1049–1051.
- Overkamp, K. E., Langklotz, S., Aras, M., Helling, S., Marcus, K., Bandow, J. E., Hoef-Emden, K., & Frankenberg-Dinkel, N. (2014). Chromophore composition of the phycobiliprotein Cr-PC577 from the cryptophyte *Hemiselmis pacifica*. *Photosynthesis Research*, *122*, 293–304.
- Pastoureaud, A., Dupuy, A., Chrétiennot-Dinet, M. J., Lantoine, F., & Loret, P. (2003). Red coloration of oysters along the French Atlantic coast during the 1998 winter season: Implication of nanoplanktonic cryptophytes. *Aquaculture*, *228*, 225–235.
- Pedrós-Alió, C., Massana, R., Latasa, M., García-Cantizano, J., & Gasol, J. M. (1995). Predation by ciliates on a metalimnetic *Cryptomonas* population: Feeding rates, impact and effects of vertical migration. *Journal of Plankton Research*, *17*, 2131–2154.
- Rathbone, H. W. (2021). Tracing the evolutionary history of the cryptophyte light harvesting antenna: A structural perspective. [Doctoral dissertation, School of Physics, University of New South Wales].
- Rathbone, H. W., Laos, A. J., Michie, K. A., Iranmanesh, H., Bizaik, J., Goodchild, S. C., Thordarson, P., Green, B. R., & Curmi, P. M. G. (2023). Molecular dissection of the soluble photosynthetic antenna from the cryptophyte alga *Hemiselmis andersenii*. *Communications Biology*, *6*, 1–15.
- Rathbone, H. W., Michie, K. A., Landsberg, M. J., Green, B. R., & Curmi, P. M. G. (2021). Scaffolding proteins guide the evolution of algal light harvesting proteins. *Nature Communications*, *12*, 1890.
- Richardson, T. L. (2022). The colorful world of cryptophyte phycobiliproteins. *Journal of Plankton Research*, *44*(6), 814–826.
- Scholes, G. D., Mirkovic, T., Turner, D. B., Fassio, F., & Buchleitner, A. (2012). Solar light harvesting by energy transfer: From ecology to coherence. *Energy and Environmental Science*, *5*, 9374.
- Spangler, L. C., Yu, M., Jeffrey, P. D., & Scholes, G. D. (2022). Controllable phycobilin modification: An alternative photoacclimation response in cryptophyte algae. *ACS Central Science*, *8*(3), 340–350.
- Stewart, D. E., & Farmer, F. H. (1984). Extraction, identification, and quantitation of phycobiliprotein pigments from phototrophic plankton. *Limnology and Oceanography*, *29*, 392–397.
- Stomp, M., Huisman, J., Stahl, L. J., & Matthijs, H. C. P. (2007). Colorful niches of phototrophic microorganisms shaped by vibrations of the water molecule. *ISME Journal*, *1*, 271–282.
- Stomp, M., Huisman, J. L., Vörös, L., Pick, F. R., Laamanen, M., Haverkamp, T., & Stahl, L. J. (2007). Colourful coexistence of red and green picocyanobacteria in lakes and seas. *Ecology Letters*, *10*, 290–298.
- Vesk, M., & Jeffrey, S. W. (1977). Effect of blue-green light on photosynthetic pigments and chloroplast structure in unicellular marine algae from six classes. *Journal of Phycology*, *13*, 280–288.
- Wedemayer, G. J. (1996). Cryptomonad biliproteins: Bilin types and locations. *Photosynthesis Research*, *48*(1–2), 163–170.
- Wedemayer, G. J., Kidd, D. G., Wemmer, D. E., & Glazer, A. N. (1992). Phycobilins of cryptophyte algae—occurrence of dihydrobiliverdin and mesobiliverdin in cryptomonad biliproteins. *Journal of Biological Chemistry*, *267*, 7315–7331.

How to cite this article: Merritt, K. A., & Richardson, T. L. (2024). Variability in spectral absorption within cryptophyte phycobiliprotein types. *Journal of Phycology*, *00*, 1–13. <https://doi.org/10.1111/jpy.13439>